C-axial oriented $(Bi_{1.5}Zn_{0.5})(Zn_{0.5}Nb_{1.5})O_7$ thin film grown on Nb doped $SrTiO_3$ substrate by pulsed laser deposition

L Z Cao[1], W Y Fu[1], S F Wang[2], Q Wang[3], Z H Sun[1], H Yang[1], B L Cheng[1], H Wang[3] and Y L Zhou[1,4]

[1] Beijing National Laboratory for Condensed Matter Physics, Institute of Physics, Chinese Academy of Sciences, Beijing 100080, People's Republic of China

[2] Physics and Technology College, Hebei University, Baoding 071002, People's Republic of China

[3] Electronic Materials Research Laboratory, Key Laboratory of the Ministry of Education, Xi'an Jiaotong University, Xi'an 710049, People's Republic of China

E-mail: ylzhou@aphy.iphy.ac.cn

Abstract
A c-axial oriented $(Bi_{1.5}Zn_{0.5})(Zn_{0.5}Nb_{1.5})O_7$ thin film has been grown on a
$(0\,0\,1)$ Nb doped $SrTiO_3$ substrate by pulsed laser deposition. The
permittivity, dielectric loss and tunability of the c-axial oriented film are
187, 0.002 and 6% (at $750\,kV\,cm^{-1}$ biasing), respectively, indicating a
figure of merit of 30. Moreover, an asymmetry behaviour is observed in the
dc electric field dependence of permittivity, which could be attributed to the
asymmetry of top and bottom electrodes.

(Some figures in this article are in colour only in the electronic version)

1. Introduction

In the past few years, much attention has been focused on the applications of dielectric thin films for tunable microwave devices, such as tunable filters, phase shifters and resonators. In practical tunable devices, the dielectric thin films must meet several critical requirements, including low dielectric loss, adequate tunability and low leakage current [1]. $Ba_{1-x}Sr_xTiO_3$ (BST) films have been widely studied for its applications in tunable devices [2–5]. However, the large dielectric loss and intrinsic hysteresis in the microwave region prevent it from further application [6]. Currently, a paraelectric material, $(Bi_{1.5}Zn_{0.5})(Zn_{0.5}Nb_{1.5})O_7$ (BZN), has been demonstrated as a potential candidate for microwave applications due to its very low dielectric loss, medium permittivity and reasonable voltage tunability [7–10]. Several deposition methods such as rf sputtering, metal organic decomposition (MOD), metal organic chemical vapour deposition (MOCVD)

and pulsed laser deposition (PLD) have been explored to deposit BZN films [7, 8, 11–16]. Compared with other deposition methods, PLD has the advantages of high deposition rate and precision in stoichiometric control. However, only a few researchers have deposited BZN films by the PLD technique up to now [11,15]. Commonly, most of the previous works were limited to the growth of polycrystalline BZN films on substrates such as Pt/vycor glass, $Pt/TiO_2/SiO_2/Si$ and Pt/Al_2O_3. Recently, Okaura *et al* reported the growth of (1 1 1)-oriented BZN films on the (1 1 1) $Pt/(001)Al_2O_3$ substrates by the MOCVD method [17], but there is no report on the growth of the (0 0 1) oriented BZN thin film as yet.

In this paper, we report the growth of c-axial oriented BZN thin films on 1% Nb doped $SrTiO_3$ (0 0 1) single crystals (STON) by PLD and its relevant dielectric properties. The c-axial oriented BZN film exhibits a permittivity of 187, a dielectric loss of 0.002 and a tunability of 6% (at $750\,kV\,cm^{-1}$ biasing), indicating a figure of merit (FOM) of 30. Moreover, an asymmetry behaviour is observed in the dc electric field dependence of permittivity, which could be attributed to the

[4] Author to whom any correspondence should be addressed.

influence of a built-in electric field in the thin film caused by the asymmetry of top and bottom electrodes.

2. Experimental

The BZN ceramic target used in this experiment was fabricated by a conventional ceramic technology as described elsewhere [18]. The (0 0 1) STON substrate (Hefei Kejing Mater. Tech. Co., Ltd, China) was $3 \times 5 \times 0.5$ mm^3 in size and serves as the bottom electrode due to its metallic conductivity. Moreover, the STON substrate has a good lattice match with the BZN thin film, which will be described in detail later. The ceramic target was mounted on a motor-driven rotary stand rotating at a constant speed to ensure a uniform ablation, and the substrates were placed parallel to the target at a distance of 45 mm. A 308 nm XeCl excimer laser with laser energy density of about 2 J cm^{-2} was used to ablate the ceramic target. BZN thin films were deposited at different temperatures with the oxygen pressure ranging from 10^{-2} to 100 Pa. It was found that the deposition temperature and oxygen pressure have a great influence on the quality of the films. When the films are deposited at a temperature lower than 500 °C, the films are amorphous and become polycrystalline after post-annealing at a high temperature. When the films are deposited under oxygen pressure lower than 1 Pa at a temperature of 700 °C, the energy dispersive x-ray analysis (EDX) measurement indicates that the BZN films suffer from Bi and Nb deficiencies due to the relatively high volatility of the two elements.

The *c*-axial oriented BZN thin films were grown at 700 °C under oxygen pressure of 30 Pa, followed by a post-annealing process at 550 °C for 20 min in 1 atm O$_2$. For comparison, we deposited the BZN films on the Pt/TiO$_2$/SiO$_2$/Si substrates with the same experimental conditions as mentioned above. The BZN films were also deposited at 400 °C on a STON substrate under oxygen pressure of 10 Pa, with a post-annealing process at 750 °C for 20 min in 1 atm O$_2$.

The thickness of all the BZN films was 200 nm measured by a surface profiler of Dektak 8. The EDX measurements revealed that the stoichiometry of the BZN films is nearly the same as that of the target. The crystal structure of the BZN films was analysed by x-ray diffraction (XRD, Mac Science M18AHF) using CuKα radiation with a scan step of 0.01° and a scan speed of 10° min^{-1}. The EDX analysis system works as an integrated feature of a scanning electron microscope (FEI, XL30 S-FEG). The surface morphologies of the BZN films were tested with Nano Scope IIIa-D3000 AFM. Dielectric measurements were taken by an Agilent 4294A precision impedance analyzer, using a parallel-plate capacitor structure with 100 nm-thickness of Pt top electrode.
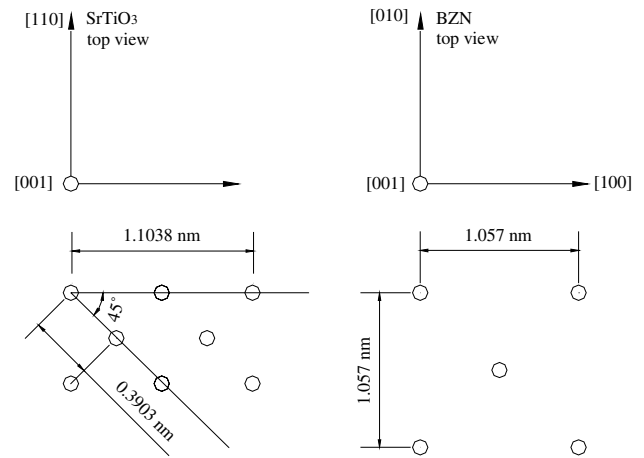
3. Results and discussion

Figure 1 shows the XRD pattern of the BZN film deposited at 700 °C and 30 Pa O$_2$ on (0 0 1) STON by PLD. Based on Lotgering's theory [19], the orientation factor can be defined as

$$F = (P - P0)/(1 - P0), \qquad (1)$$

$$P = \sum I(abc) / \sum I(hkl), \qquad (2)$$
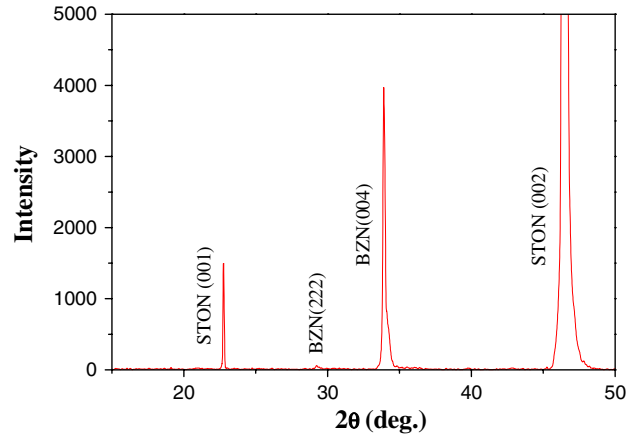
**Figure 1.** XRD patterns of *c*-axial oriented BZN film on the (0 0 1) STON substrates.

Figure 2. Schematic diagram of the oriented growth of BZN films on the (0 0 1) STON substrate.

where F denotes the orientation factor with respect to a reference plane (abc) where (abc) denotes the Miller indices, P represents the ratio of the sum of intensities of the interested family of planes (abc) to the sum of all reflections and P_0 stands for the equivalent ratio for ceramic powder of the target with random orientation. The value of the orientation factor for the preferred orientation is in the range from 0 to 1. $F = 0$ denotes a film with random orientation and $F = 1$ denotes a completely oriented film. The orientation factor of this BZN thin film calculated from the XRD pattern is 0.975, indicating a good *c*-axial preferred orientation of the BZN thin film.

The BZN has a cubic pyrochlore structure with space group $Fd3m$ [9] and $a = 1.057$ nm, while STON belongs to a cubic perovskite structure with space group $Fm3m$ and $a = 0.3903$ nm. As shown in figure 2, the lattice of BZN matches well with that of the STON in its cater-cornered orientation. The lattice mismatch between the BZN films and the STON substrate is less than 4.3% and the lattice of the BZN film undergoes a biaxial compressive stress. Such a match in lattice may be responsible for the *c*-axial oriented growth of BZN films on the (0 0 1) STON substrate at a high temperature.

However, both the film deposited at 400 °C on the STON substrate and the film deposited at 700 °C on
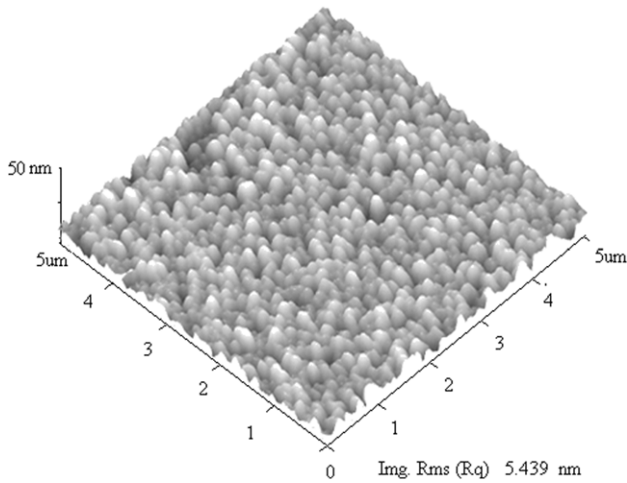
**Figure 3.** AFM images of the *c*-axial oriented BZN thin film.

the Pt/TiO$_2$/SiO$_2$/Si substrate showed random oriented polycrystalline structure. The XRD results are consistent with those reported by Lu and coworkers, which are not shown here [20, 21].

Figure 3 is the surface morphology of the *c*-axial oriented BZN film via the tapping mode AFM. The BZN film is crack free with a root-mean-square surface roughness (RMS) of 5.4 nm and a grain size around 150 nm. These parameters are consistent with those reported by other research groups [8, 11].

Figure 4(*a*) shows the permittivity and dielectric loss of the *c*-axial oriented BZN film as a function of frequency ranging from 10 kHz to 1 MHz with an ac oscillation voltage of 400 mV. For comparison, the dielectric behaviour of the random oriented polycrystalline BZN film grown at 400 °C on the STON substrate is given in figure 4(*b*). At the frequency of 10 kHz, the permittivity and dielectric loss are 186 and 0.002 and 204 and 0.008 for the *c*-axial oriented BZN film and the random oriented polycrystalline one, respectively. The dielectric loss of the *c*-axial oriented thin film is much lower than that of the random oriented thin film. The permittivity of both films almost keeps a constant value, while the loss tangent increases obviously with increasing frequency. Such an increase in the loss tangent that is acccompanied by a constant value of permittivity should be attributed to the conductor losse's contribution of the metallic electrode [12].

The permittivity versus the bias electric field of the BZN films measured at 10 kHz with an ac oscillation voltage of 400 mV is illustrated in figure 5. At a bias electric field of 750 kV cm^{-1}, a tunability of 6% is obtained for the *c*-axial oriented BZN film and of 8% for the random oriented polycrystalline BZN film with the same substrate. A tunability of 55% has been reported for the BZN films on the Pt/Al$_2$O$_3$ substrates by Lu and Stemmer [12]. The maximum electric field was 2.4 MV cm^{-1} in their work and is only 0.75 MV cm^{-1} in our experiment. Here we expect higher tunability with increasing applied dc electric field.

In figure 5, it is noted that the bias electric field E_m at which the permittivity has its maximum value is not located at the zero bias electric field, but shifts towards the negative bias region for both samples. However, this asymmetry phenomenon is not observed for the BZN film deposited on the Pt/TiO$_2$/SiO$_2$/Si
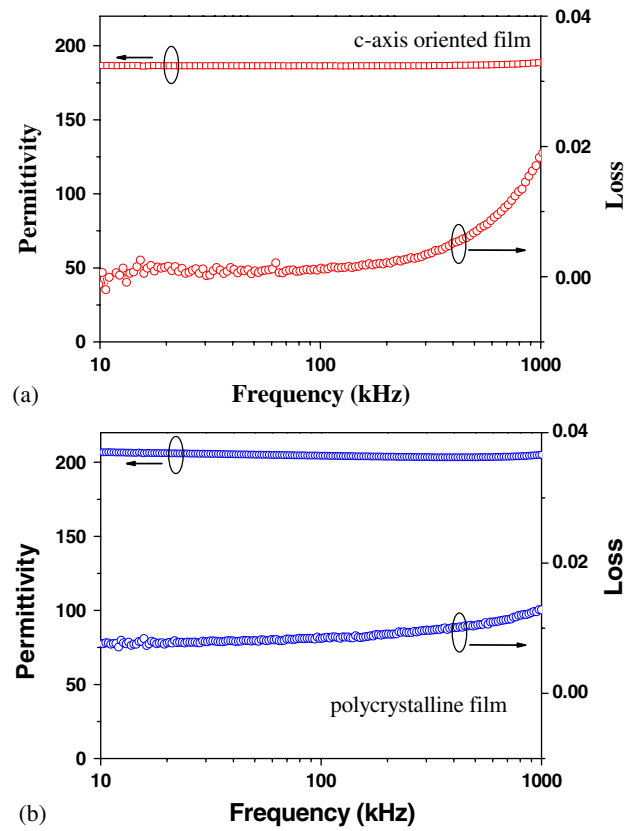

Figure 4. Permittivity and dielectric loss as a function of frequency for (*a*) *c*-axial oriented and (*b*) random oriented polycrystalline BZN films.
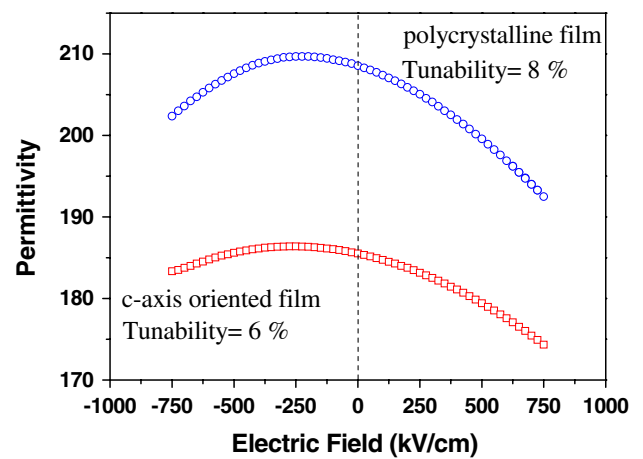
Figure 5. Dependence of permittivity on the dc electric field at 100 kHz in the range from −750 to 750 kV cm^{-1} for BZN films.

substrate which has the same top and bottom electrodes. Therefore, the asymmetry may result from the asymmetry of the top and bottom electrodes. As discussed by many researchers, an interfacial layer exists between the dielectric film and the electrode, and a built-in electric field could be formed at the interfacial layer [22–24]. For a Pt/BZN/Pt capacitor, the built-in electric fields formed on the top and bottom electrodes could counteract each other. But, for a Pt/BZN/STON capacitor, there are two different interfacial layers formed on the top and bottom electrodes, and then the
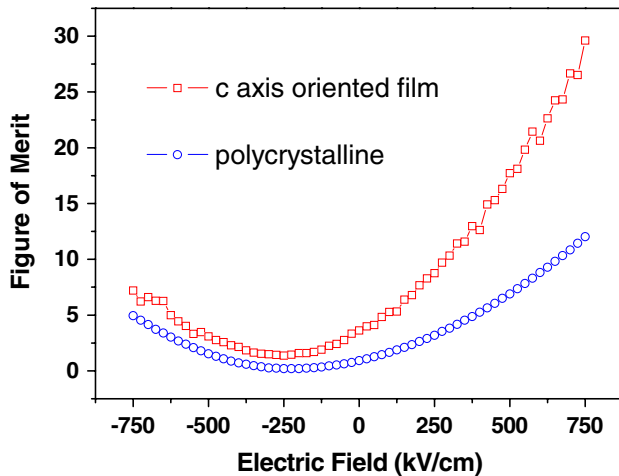
Figure 6. The FOM as a function of the bias electric field for the BZN films.

built-in electric fields could not counteract each other. So the built-in electric field should be the origin of the asymmetric behaviour, because the applied electric field on the BZN film capacitor must overcome the effect of the built-in electric field. This theory provides only qualitative explanation for the observed trend in the *C*–*V* measurements and further investigation work is required.

In a tunable microwave device, the quality of the film is evaluated by FOM defined as

$$\text{FOM} = \left(\frac{\text{tunability}}{\tan \delta} \right) = \left\{ \frac{[\varepsilon(0) - \varepsilon(E_{\max})]/\varepsilon(0)}{\tan \delta} \right\}. \quad (3)$$

As shown in figures 5 and 6, the *c*-axial oriented BZN film has a maximum FOM of 30 with the low dielectric loss of 0.002 and a tunability of 6%. The random oriented polycrystalline BZN film exhibits a relatively lower FOM of 11 because of a high loss of 0.01. The result indicates that the *c*-axial oriented film exhibits better dielectric properties than the random oriented polycrystalline one. Moreover, dielectric properties of the *c*-axial oriented BZN films are also better than that of the optimized doped BST films on the STON substrates, which have a FOM of 23 at the same bias electric field [25].

4. Conclusions

In summary, we fabricated a *c*-axial oriented BZN film on the STON substrate by PLD methods. The *c*-axial oriented BZN film exhibits a permittivity of 187, a dielectric loss of 0.002 and a tunability of 6%. Consequently, a FOM of 30 is obtained, which is much better than that of the random oriented polycrystalline BZN films. Furthermore, an asymmetry characteristic is observed in the electric field-dependent permittivity, which may result from the asymmetry of top and bottom electrodes.

The experimental results indicate that BZN films are an attractive prospect for tunable microwave device application.

Future work will be focused on the fabrication of epitaxial BZN films with different orientations to investigate the influence of orientation on dielectric properties.

Acknowledgments

References

[1] Cole M W, Joshi P C and Ervin M H 2001 *J. Appl. Phys.* **89** 6336
[2] Jin F, Auner G W, Naik R, Schubring N W, Mantese J V, Catalan A B and Micheli A L 1998 *Appl. Phys. Lett.* **73** 2838
[3] Ngo E, Joshi P C, Cole M W and Hubbard C W 2001 *Appl. Phys. Lett.* **79** 248
[4] Chang W T, Gilmore C M, Kim W J, Pond J M, Kirchoefer S W, Qadri S B, Chirsey D B and Horwitz J S 2000 *J. Appl. Phys.* **87** 3044
[5] Streiffer S K, Basceri C, Parker C B, Lash S E and Kingon A I 1999 *J. Appl. Phys.* **86** 4565
[6] Ha S, Lee Y S, Hong Y P, Lee H Y, Lee Y C, Ko K H, Kim D W, Hong H B and Hong K S 2005 *Appl. Phys. A Mater.* **80** 585
[7] Hong Y P, Ha S, Lee H Y, Lee Y C, Ko K H, Kim D W, Hong H B and Hong K S 2002 *Thin Solid Films* **419** 183
[8] Ren W, Trolier-McKinstry S, Randall C A and Shrout T R 2001 *J. Appl. Phys.* **89** 767
[9] Wang H, Elsebrock R, Schneller T, Waser R and Yao X 2004 *Solid State Commun.* **132** 481
[10] Wang X L, Wang H and Yao X 1997 *J. Am. Ceram. Soc.* **80** 2745
[11] Jiang S W, Jiang B, Liu X Z and Li Y R 2006 *J. Vac. Sci. Technol.* A **24** 261
[12] Lu J W and Stemmer S 2003 *Appl. Phys. Lett.* **83** 2411
[13] Park J, Lu J W, Stemmer S and York R A 2005 *J. Appl. Phys.* **97** 084110
[14] Park J, Lu J W, Stemmer S and York R A 2005 *Integr. Ferroelectr.* **77** 21
[15] Cheng H F, Chen Y C and Lin I N 2000 *J. Appl. Phys.* **87** 479
[16] Kim J Y, Kim D W, Jung H S and Hong K S 2005 *Japan. J. Appl. Phys. Part 1* **44** 6648
[17] Okaura S, Suzuki M, Okamoto S, Uchida H, Koda S and Funakubo H 2005 *Japan. J. Appl. Phys. Part 1* **44** 6957
[18] Wang H and Yao X 2001 *J. Mater. Res.* **16** 83
[19] Lotgering F K 1959 *J. Inorg. Nucl. Chem.* **9** 113
[20] Lu J W, Klenov D O and Stemmer S 2004 *Appl. Phys. Lett.* **84** 957
[21] Park J, Lu J W, Stemmer S and York R A 2005 *Integr. Ferroelectr.* **77** 21
[22] Trithaveesak O, Schubert J and Buchal C 2005 *J. Appl. Phys.* **98** 114101
[23] Maruno S, Kuroiwa T, Mikami N, Sato K, Ohmura S, Kaida M, Yasue T and Koshikawa T 1998 *Appl. Phys. Lett.* **73** 954
[24] Cillessen J F M, Prins M W J and Wolf R M 1997 *J. Appl. Phys.* **81** 2777
[25] Cao L Z, Cheng B L, Wang S Y, Zhou Y L, Jin K J, Lu H B, Chen Z H and Yang G Z 2005 *J. Appl. Phys.* **98** 034106